The role of the Mg^{2+} ions in Cr^{3+} spectroscopy for near-stoichiometric $LiNbO_3$ crystals

2003 J. Phys.: Condens. Matter 15 281

(http://iopscience.iop.org/0953-8984/15/2/328)

INSTITUTE OF PHYSICS PUBLISHING JOURNAL OF PHYSICS: CONDENSED MATTER

J. Phys.: Condens. Matter **15** (2003) 281–290 PII: S0953-8984(03)52432-8

The role of the Mg^{2+} ions in Cr^{3+} spectroscopy for near-stoichiometric $LiNbO_3$ crystals

T P J Han[1,3], F Jaque[1], V Bermúdez[2] and E Diéguez[2]

[1] Department of Physics and Applied Physics, University of Strathclyde, John Anderson Building, 107 Rottenrow, Glasgow G4 ONG, UK
[2] Departamento de Fisica de Materials, Universidad Autonoma de Madrid, Cantoblanco 28049, Madrid, Spain

E-mail: t.han@strath.ac.uk

Received 15 August 2002
Published 20 December 2002
Online at stacks.iop.org/JPhysCM/15/281

Abstract

The optical spectroscopy of Cr^{3+} ions doped into near-stoichiometric $LiNbO_3$ crystals, pure and co-doped with MgO, has been investigated.

In the near-stoichiometric $LiNbO_3$:Cr(0.2 mol%):Mg(2 mol%) crystal, the optical spectra resemble those previously observed for congruent $LiNbO_3$:Cr:MgO samples when the total MgO content exceeds the 4.6 mol% threshold. The coexistence of two types of Cr^{3+} centre ($[Cr]_{Li}$ and $[Cr]_{Nb}$) characterized the optical and luminescence spectra of this sample. The concentration equilibrium between the two types of centre is strongly displaced towards the $[Cr^{3+}]_{Nb}$ centre, permitting us to obtain with accuracy the parameters of the broad bands. The R-line associated with the $[Cr]_{Nb}$ centre is only observable in the low-temperature emission spectrum. The Fano anti-resonance lines present have been observed to be more pronounced for the near-stoichiometric samples than for congruent ones.

(Some figures in this article are in colour only in the electronic version)

1. Introduction

Lithium niobate, $LiNbO_3$, is an important material for applications in electro-optics and integrated optical devices. However, it suffers from a photorefractive effect at moderately low optical excitation power. In order to increase the resistance of this material to this 'optical damage' in nonlinear applications, such as amplification and laser action or second-harmonic generation, most $LiNbO_3$ crystals are usually intentionally doped with a small but significant amount of MgO, ∼5–6 mol% [1]. Recently it has been reported that the same effect can be archived with ZnO [2] and Sc_2O_3 [3]. The presence of these cations is an additional source

[3] Author to whom any correspondence should be addressed.

of disorder within the host lattice and could affect the properties of the optically active dopant ions.

The Cr^{3+} ion has been demonstrated to be a useful optical and paramagnetic probe for studying the location of the doped cations in $LiNbO_3$ crystals. It has been reported that in congruent $LiNbO_3$:Cr samples (where the Li/Nb ratio is 0.946) co-doped with low concentrations, less than 4.5 mol%, of MgO and ZnO, the predominant Cr^{3+} centre is the unperturbed Cr^{3+} ion located in the Li^+ vacancy, $[Cr^{3+}]_{Li}$-γ (the γ-centre). The optical absorption spectrum associated with this centre consists of two broad bands ascribed to the vibronic radiative transitions $^4A_2 \rightarrow {}^4T_1$ and $^4A_2 \rightarrow {}^4T_2$. In addition to these broad bands, a narrow line associated with the $^4A_2 \rightarrow {}^2E$ zero-phonon transition (the R-line) is also observed. For cation concentrations greater than 4.5 mol%, an additional new Cr^{3+} centre has been detected in both optical and electron paramagnetic resonance (EPR) spectra [4, 5]. This centre has been assigned to Cr^{3+} ions substituting into the Nb^{5+} sites, charge compensated and perturbed by a nearby Mg^{2+} ion, $[Cr]_{Nb}$ [6, 7]. The broad $^4A_2 \rightarrow {}^4T_2$ and $^4A_2 \rightarrow {}^4T_1$ optical absorption bands related to this centre were found to be red-shifted to lower energy in comparison with that associated with the $[Cr]_{Li}$ centre [4]. Because of the overlap between the absorption bands associated with the $[Cr]_{Li}$-γ and $[Cr]_{Nb}$ centres, the broad-band parameters of the $[Cr]_{Nb}$ centre are not well characterized. The zero-phonon $^4A_2 \rightarrow {}^2E$ transition (R-line) associated with this centre has never been observed in absorption spectra [8].

Near-stoichiometric-composition $LiNbO_3$ can be grown in 6 wt% K_2O flux using the top-seeded solution growth (TSSG) technique [9]. The perception that stoichiometric (sto-) or near-stoichiometric (nsto-) $LiNbO_3$ has far fewer intrinsic defects than its congruent counterpart gives rise to the expectation of much improved crystal quality and reduced photorefractive effect. sto-$LiNbO_3$ and nsto-$LiNbO_3$ crystals doped with Cr^{3+} ions have already been investigated [10]. However, little is known about the effect of co-doping with cations on these crystals, apart from the basic fact that the $[Cr]_{Li}$ and the $[Cr]_{Nb}$ centres coexist for low concentrations of MgO (0.2 mol% in the crystal) [11].

In this work, the optical properties, such as absorption and luminescence, of Cr^{3+} ions in nsto-$LiNbO_3$, pure and co-doped with MgO, are presented. It has been observed that under special growth conditions the coexistence of the two Cr^{3+} centres is replaced by dominance of the $[Cr^{3+}]_{Nb}$ centres. This result has permitted us to identify unambiguously the optical absorption bands associated with these centres.

2. Experimental method

nsto-$LiNbO_3$ crystals doped with 0.1 mol% of Cr_2O_3 and with 2 mol% of MgO in the melt were grown in air by the TSSG method in a K_2O flux using two different pull rates: 0.3 and 2 mm h^{-1}. The co-doped $LiNbO_3$:Cr:MgO crystal growth using the faster pull rate showed a gradual colour variation along the length of the boule: from green at the top of the boule to pink at the bottom. However, the co-doped $LiNbO_3$:Cr:MgO crystal obtained by using the slower pull rate presented a homogeneous pink colour along the length of the boule.

Optical absorption spectra in the temperature range between room temperature and 100 K were recorded with an AVIV 14DS spectrometer. Optical absorption spectra at 10 K were performed using a Varian Carey-SE spectrophotometer. The continuous-wave (cw) luminescence emission investigation was performed using the resonant line of an argon-ion laser. The emitted light was dispersed by a SPEX 500M monochromator and detected with a Hamamatsu R-2949 photomultiplier. All low-temperature measurements were obtained using a closed-cycle helium cryorefrigerator.

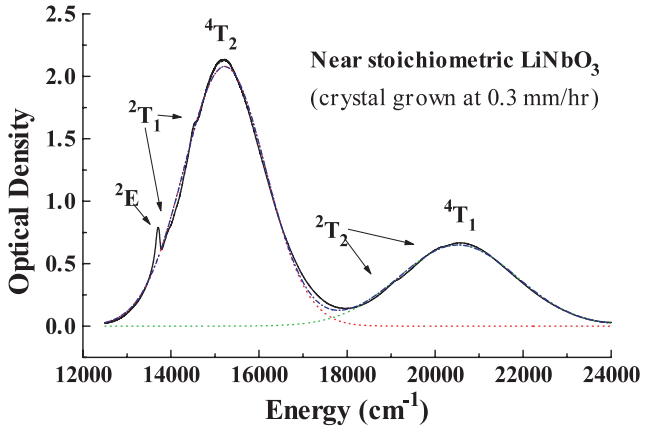

Figure 1. The absorption spectrum of a near-stoichiometric $LiNbO_3$:Cr sample at room temperature (continuous curve). The dash–dot curve corresponds to the best fit considering two Gaussian (dotted curve) bands. The relevant parameters are listed in table 1.

3. Experimental results and discussion

Figure 1 shows the unpolarized room temperature absorption spectrum of a nsto-$LiNbO_3$ sample doped with Cr^{3+} ions. The spectrum consists of two broad bands centred at 15 220 and 20 520 cm^{-1}; the low-energy band is approximately a factor of three more intense than the high-energy band. In addiction to the broad bands, a clearly defined narrow line centred at 13 320 cm^{-1} is observed as well as some less well defined peaks on the low-energy side of the two broad bands. This 13 320 cm^{-1} narrow line is clearly resolved into three peaks at low temperature. It is clear that a good fit of this absorption spectrum, neglecting the narrow line at 13 320 cm^{-1}, can be achieved by considering two Gaussian bands. The general features of this spectrum resemble those previously reported for congruent $LiNbO_3$:Cr, pure and co-doped with MgO or ZnO with concentrations less than 4.5 mol% [4, 5]. In both cases the two broad bands were assigned to the $^4A_2 \rightarrow {}^4T_2$ and $^4A_2 \rightarrow {}^4T_1$ vibronic transitions and have been ascribed to Cr^{3+} ions located in the unperturbed Li^+ site, the $[Cr]_{Li}$-γ centre (the γ-centre). The narrow line centred at 13 320 cm^{-1} has been ascribed to the $^4A_2 \rightarrow {}^2E$ (R-line) transitions and the weak structures on the low-energy side of the two broad bands are assigned to the $^4A_2 \rightarrow {}^2T_1$ and $^4A_2 \rightarrow {}^4T_2$ transitions [12]. Subsequent crystal-field calculations showed that this $[Cr]_{Li}$-γ centre has a low-crystal-field configuration where the relaxed $^4T_2$ is the lowest excited level and hence no emission from the ^2E level (R-line) is expected [11]. However, in luminescence experiments with pure and MgO co-doped samples of congruent and nsto-$LiNbO_3$:Cr crystals, two narrow emission lines centred at 13 680 and 13 610 cm^{-1} have been reported [13]. These two emissions lines were assigned to the $^2E \rightarrow {}^4A_2$ transitions (R-lines) of two perturbed Cr^{3+} centres located in Li^+ sites: the Cr^{3+} ion in the Li vacancy, $[Cr]^{V}_{Li}$-β, and the Cr^{3+} ion in the Nb antisite, $[Cr]^{Nb}_{Li}$-α (denoted as β-and α-centres respectively in the literature [8]). Both centres correspond to high-crystal-field configurations, but the exact nature of the perturbation is still unclear at present. For the nsto-$LiNbO_3$:Cr crystal, an extra narrow band centred at 13 538 cm^{-1} has been reported and has been interpreted as the zero-phonon line of the $^4T_2 \rightarrow {}^4A_2$ transition [10].

Figure 2 shows the unpolarized optical absorption spectrum of the fast-growth nsto-$LiNbO_3$:Cr:MgO sample (2 mol% of MgO in the melt). The sample was cut from the top part of the crystal and shows a uniform green colour. The spectrum consists of two broad brands with

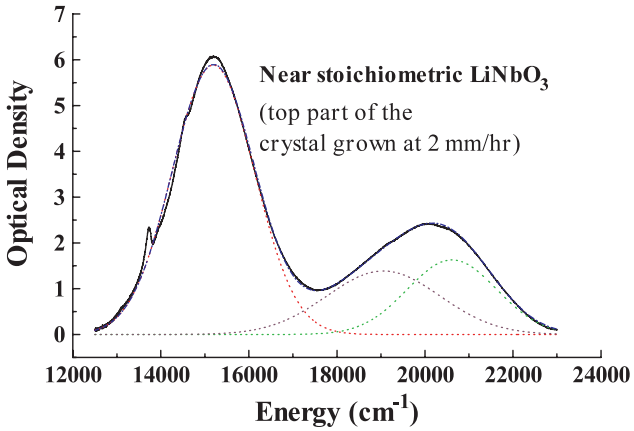

Figure 2. The room temperature absorption spectrum of the top part of the boule of a near-stoichiometric $LiNbO_3$:Cr:MgO (2%) sample grown at 2 mm h^{-1} (continuous curve). The dash–dot curve corresponds to the best fit considering three Gaussian (dotted curve) bands. The relevant parameters are listed in table 1.

similar characteristics to the nsto-$LiNbO_3$:Cr crystal, as shown in figure 1. The R-lines and the weak structures associated with the $^4T_1$ and $^4T_2$ excited levels remain unchanged. However, two noticeable differences are revealed under detail inspection: the high-energy broad band appears broadened and slightly red-shifted to lower energy; and the relative intensity of the two broad bands decreases. These two facts suggest an additional band in the 18 000–20 000 cm^{-1} region. In fact, the general features of the broad bands are best fitted by considering three Gaussian bands: the two previous broad bands observed for nsto-$LiNbO_3$:Cr samples and a new broad band centred at ∼18 900 cm^{-1}. A similar change in the absorption spectra was previously observed for congruent $LiNbO_3$:Cr crystals co-doped with MgO and ZnO for concentrations close to the threshold doping level of 4.5 mol% [4, 5].

The sample cut from the bottom part of the boule shows a uniform pink colour and its absorption spectrum at room temperature is presented in figure 3. The spectrum consists of two broad bands and the comparison with the green sample reveals the following differences:

(i) the high-energy broad bands appear red-shifted to lower energy;
(ii) the low-energy broad band is broadened on the longer-wavelength side; and
(iii) the relative intensities of the two broad bands are similar.

The general features of the broad band are now best described by considering four Gaussian bands. Two of the bands are centred at positions close to those found for the nsto-$LiNbO_3$:Cr sample, associated with $[Cr]_{Li}$ centres, but with different relative intensities. The third band is centred at 18 600 cm^{-1}, close to the position observed for the nsto-$LiNbO_3$:Cr:MgO sample (fast growth) as presented in figure 2. The fourth band, centred at 13 443 cm^{-1}, presents a weak absorption and therefore the fitting should be considered as a first approximation. The absorption spectrum displayed in figure 3 resembles very strongly that found for congruent $LiNbO_3$:Cr crystals co-doped with MgO and ZnO cations with concentrations above the threshold level [4, 5].

For congruent co-doped samples it has been reported that the change detected in the optical spectrum is accompanied by the presence of a new isotropic EPR line. This EPR line appears suddenly when the MgO or ZnO concentration crosses the threshold value [4, 5] and has been ascribed to a new Cr^{3+} centre located in the Nb^{5+} site, $[Cr]_{Nb}$ [5, 6]. The isotropic

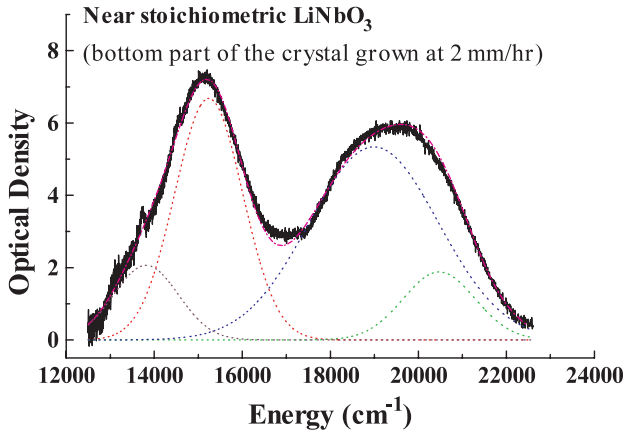

Figure 3. The room temperature absorption spectrum of the bottom part of the boule of a near-stoichiometric $LiNbO_3$:Cr:MgO (2%) sample grown at 2 mm h^{-1} (continuous curve). The dash–dot curve corresponds to the best fit considering four Gaussian (dotted curve) bands. The relevant parameters are listed in table 1.

characteristic of this centre was explained by considering that the proximity of the Mg^{2+} ions shifts the Cr^{3+} ions to a more centred position, leading to a near-cubic crystal field. The emergence of this new Cr^{3+} site was explained assuming that the Cr^{3+}-ion redistribution is induced by the presence Mg^{2+} or Zn^{2+} ions in the sample [4, 5]. In the two accepted cation substitution models for congruent $LiNbO_3$(Li/Nb = 0.945) crystal, the Li^+-and Nb^{5+}-vacancy models [13, 14], the total concentration of Li^+ vacancies or antisites is ∼4.6 mol%. Assuming that divalent cations are preferentially entering into the Li^+ vacancies or antisites [4], for Mg^{2+}- or Zn^{2+}-ion concentrations above ∼4.5 mol%, all Li^+ vacancies or antisites are expected to be filled. Under this condition, Cr^{3+} ions can be substituted at intrinsic Li^+ sites and Nb^{5+} sites and both the $[Cr]_{Li}$ and $[Cr]_{Nb}$ centres are present in the crystal.

Figure 4 shows the unpolarized absorption spectrum of a slow-growth nsto-$LiNbO^3$:Cr:MgO sample at room temperature. The crystal has a homogeneous pink colour along the full length of the boule. The absorption spectrum of this sample consists of two broad bands centred at 19 000 and 14 000 cm^{-1}, a weak narrow line peaked at 13 700 cm^{-1} and a weak structure located closed to the peak of the low-energy broad band. This spectrum has general features very similar to those of the spectrum presented in figure 3, for the bottom part of the boule of the fast-growth nsto-$LiNbO_3$:Cr:MgO sample, with the exception that the intensity of the higher-energy band is now much larger than that of the low-energy band. This change of the intensity ratio between the two bands has also been observed, but to a lesser extent, in congruent samples co-doped with either divalent or trivalent cations at concentrations above the threshold level. The general features can be readily fitted with four Gaussian bands. The calculated peak position of each band is within 5% for the four spectra and they are very close to those reported for congruent $LiNbO_3$ samples [4, 5]. The two calculated bands, A and B, are associated with the $^4A_2 \rightarrow {}^4T_2$ and $^4A_2 \rightarrow {}^4T_1$ transitions of the $[Cr]_{Li}$ centres respectively and their relative intensity ratio is maintained within 10% for the four spectra. The other two bands, C and D, are associated with the $[Cr]_{Nb}$ centre and their relative intensity ratio is the opposite of that for A and B. The fitted parameters for figures 1–4 are presented in table 1.

It is important to note that in the nsto-$LiNbO_3$:Cr:MgO sample (slow growth) the concentration threshold that marks the coexistence of the two Cr^{3+} centres is found for a

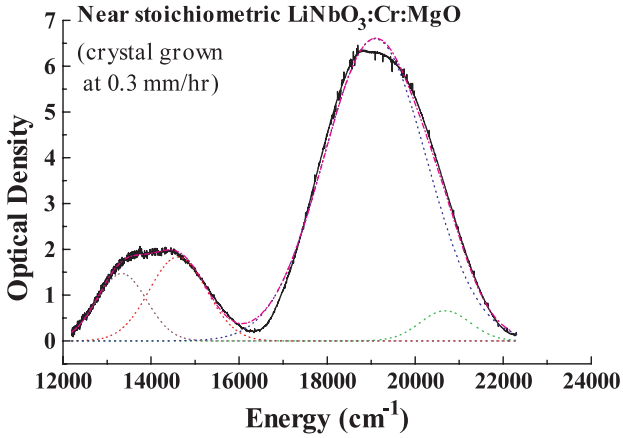

Figure 4. The room temperature absorption spectrum of a near-stoichiometric $LiNbO_3$:Cr:MgO (2%) sample grown at 0.3 mm h^{-1} (continuous curve). The dash–dot curve corresponds to the best fit considering four Gaussian (dotted curve) bands. The relevant parameters are listed in table 1.

Table 1. Parameters for the Gaussian fit as presented in figures 1–3. The Gaussian formula used is $\sum_i a_{0i} \exp[-0.5(\frac{x-a_{1i}}{a_{2i}})^2]$, where a_{0i} = amplitude, a_{1i} = centre and a_{2i} = width.

Parameters	Figure 1	Figure 2	Figure 3	Figure 4
A				
Amplitude	2.08	0.59	0.07	0.18
Centre (cm^{-1})	15 222	15 193	15 239	14 612
Width (cm^{-1})	928	934	774	651
B				
Amplitude	0.65	0.16	0.02	0.07
Centre (cm^{-1})	20 519	20 616	20 474	20 681
Width (cm^{-1})	1338	1014	818	571
C				
Amplitude		0.14	0.05	0.66
Centre (cm^{-1})		19 056	18 991	19 089
Width (cm^{-1})		1286	1470	1165
D				
Amplitude			0.02	0.15
Centre (cm^{-1})			13 814	13 335
Width (cm^{-1})			736	565

MgO concentration of 2 mol% whereas the concentration is ∼4.5 mol% for the corresponding congruent sample. For near-stoichiometric crystals, a lower Li^+-vacancy concentration (Li vacancy and antisite) than in congruent crystals is expected. Hence, it is not surprising that the critical Mg^{2+}-ion content necessary for the creation of the $[Cr]_{Nb}$ centre should be smaller.

The change of colour observed along the length of the fast-growth crystal (from green to pink) could be interpreted as due to a gradual change of the crystal's composition from the top to the bottom of the crystal. The spectroscopic results for the sample from the top of the boule (green) resemble those for congruent crystals, whereas those for the pink sample from the bottom of the boule are close to those for near-stoichiometric and congruent samples with cation concentrations above the threshold. The present experimental result is unable to distinguish

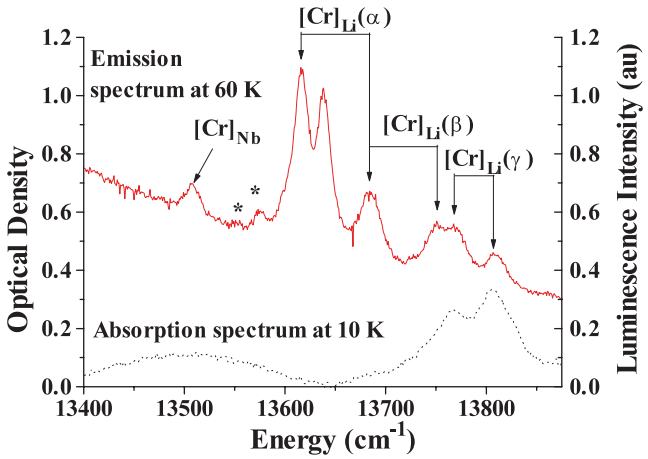

Figure 5. 60 K photoluminescence spectra of a near-stoichiometric $LiNbO_3$:Cr:MgO sample (0.3 mm h^{-1} growth rate) obtained by excitation at 514.5 nm (continuous curve). The absorption spectrum of the same sample recorded at 10 K (dotted curve) is also shown. ∗: unidentified peaks.

between these two types of crystal. At the relatively fast growth rate of 2 mm h^{-1}, the crystal has insufficient time to establish the growth conditions for stoichiometric composition and grows in its more stable congruent composition. However, the growth conditions continue to change during the growth process because the melt becomes K^+ rich and thus the flux concentration changes; hence it is to be expected that the crystal composition will change as well. The precise nature of this change is not known, but the increase of the ratio between the K_2O flux and the $LiNbO_3$ melt means that it is most likely to shift the crystal composition towards stoichiometric [9]. It is also not unreasonable to expect the distribution coefficient of MgO also to change with the crystal's composition. It has been shown for Zn doped in congruent $LiNbO_3$ that the distribution coefficient varies depending on the Zn concentration in the melt (it is 1 below the threshold of ∼4.5 mol% and less than 1 above the threshold) [16].

Despite the fact that the optical absorption spectrum of the nsto-$LiNbO_3$:Cr:MgO sample, figure 4, is basically dominated by [Cr]Nb centres, only the R-line corresponding to the [Cr]Li-γ centres was detected at room temperature. Figure 5 shows the emission spectrum of the nsto-$LiNbO_3$:Cr:MgO sample (slow growth) in the 13 400–13 800 cm^{-1} region under 19 436 cm^{-1} argon-ion laser line excitation at 60 K together with the 10 K absorption spectrum. It clearly shows that in absorption only the R-lines of the [Cr]Li-γ centre are observable, whereas in emission the R-lines of all the major Cr centres are revealed. The emission lines and their assigned centres reported in the literature are indicated in the figure. The structures observed near the peak of the broad bands, in figure 4, resemble dips similar to those associated with Fano anti-resonance lines [17]. The energy position of the R-lines and the fitted broad band (table 1) for the $[Cr]_{Nb}$ centre are red-shifted with respect to the $[Cr]_{Li}$ centres. This, according to Tanabe–Sugano theory, indicates that the $[Cr]_{Nb}$ centre has a weaker crystal-field strength than the $[Cr]_{Li}$ centres. In fact, Biernacki *et al* [18] suggested that because of the different charge states of the Cr^{3+} ion compared with those of Li^+ and Nb^{5+}, the electrostatic interaction most probably forces the oxygen ligands to relax inwardly for $[Cr]_{Li}$ centres and outwardly for $[Cr]_{Nb}$ ones.

The low-temperature, 10 K, absorption spectrum of the slow-growth nsto-$LiNbO_3$:Cr:MgO sample is shown in figure 6. The splitting of the R-lines associated with the

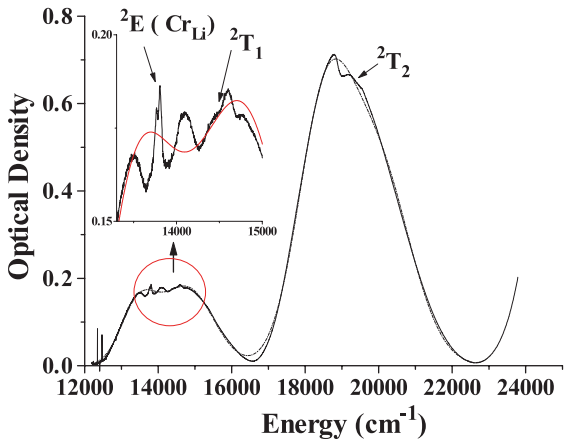

Figure 6. The 10 K absorption spectrum of a near-stoichiometric $LiNbO_3$:Cr:MgO (2%) sample (0.3 mm h^{-1} growth rate). The dotted curve corresponds to the best fit considering four Gaussian bands.

Table 2. Parameters for the anti-resonance fit using equation (1) in the text. The best-fit curve is shown in figure 7.

	Oscillator 1	Oscillator 2	Oscillator 3
$\hbar\omega_0$ (cm^{-1})	14 177	14 665	18 940
ξ	67	61	80
q	−1.9	−0.75	−0.38
p	0.016	0.030	0.050

$[Cr]_{Li}$-γ centre is well resolved. The dips near the peaks of the bands are now clearly defined and resemble the characteristics of Fano anti-resonance lines. These anti-resonance lines are observed when a sharp absorption line of an impurity centre is overlapped by a broad vibronic band (considered as a quasi-continuum state). In the case of the Cr^{3+} ions, it has been reported that there are Fano anti-resonances between the sharp levels (^2E, $^2T_1$ and $^2T_2$) and the broad vibronic excited levels $^4T_2$ and $^4T_1$, via the spin–orbit interaction [16, 19]. In the present case, the Dq/B parameter value calculated for the Cr^{3+} centres [12, 13] is close to the crossover point in the Sugano and Tanabe diagram and therefore a possible overlapping/interaction between ^2E, $^2T_1$ and $^2T_2$ sharp levels and the quasi-continuum $^4T_2$ and $^4T_1$ levels is to be expected. Figure 7 shows the ratio $R(\omega) = \alpha(\omega)/\alpha_B(\omega)$ for the anti-resonance features observed in the 14 400 cm^{-1} region. $\alpha(\omega)$ is the absorption coefficient (experiment) and $\alpha_B(\omega)$ is the absorption coefficient of the continuum (calculated curve). According to Fano theory, in the notation used by Sturge and Guggenheim [19], the ratio $R(\omega)$ in the vicinity of an isolated resonance is given by

$$R(\omega) = 1 + p\frac{q^2 + 2\xi q - 1}{1 + \xi^2} \tag{1}$$

where the parameters p, q, ξ are the same as those defined by Sturge and Guggenheim [19]. The calculated parameters presented in table 2 are in acceptable agreement with those for other d^3-ion systems [17, 19].

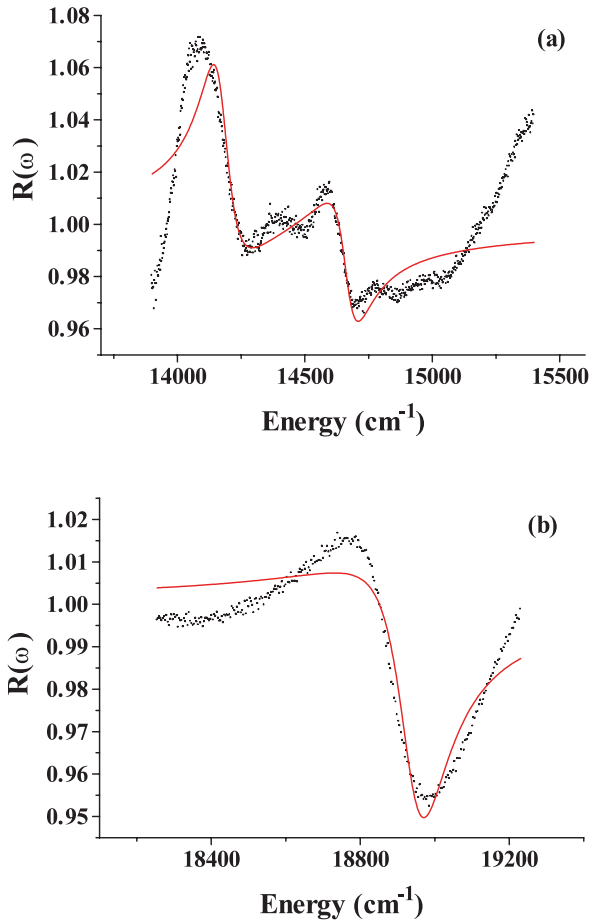

Figure 7. Dots represent the ratio $R(\omega)$ obtained from figure 6. The solid curve is the best fit using equation (1) in the text, taking into account two anti-resonances for: (a) the region 13 700–15 700 cm^{-1}; (b) the region 18 400–19 200 cm^{-1}.

4. Conclusions

In summary, the role of the Mg ions in the optical properties of nsto-$LiNbO_3$:Cr:MgO can be summarized as follows.

The presence of Mg^{2+} ions induces the coexistence of two types of Cr^{3+} centre located in Li^+ and Nb^{5+} sites in a similar way to that observed in congruent samples. However, in near-stoichiometric crystals the MgO critical concentration level for the Cr^{3+}-centre redistribution is markedly lower, at $\sim$2 mol%. The general features of the absorption spectrum of the nsto-$LiNbO_3$:Cr:MgO sample are dominated by the $[Cr]_{Nb}$ centre. The presence of Fano anti-resonance lines is more pronounced for the near-stoichiometric than for the congruent samples.

The growth rate of near-stoichiometric crystals is critical for achieving a composition as close to stoichiometric as possible.

Acknowledgments

FJ, VB and ED would like to acknowledge the support of the Ministerio de Educacion y Cultura (Spain). TPJH would like to acknowledge the financial support of the EPSRC.

References

[1] Zhong G, Jian J and Wu Z 1980 *Proc. 11th Int. Quantum Electronics Conf.* (Washington, DC: Optical Society of America) p 631
[2] Volk T R, Pryalkin V I and Runinina N M 1990 *Opt. Lett.* **15** 996
[3] Volk T, Runinina N and Wöhleke M 1986 *J. Opt. Soc. Am.* B **3** 140
[4] Diaz-Caro J, García-Sole J, Bravo D, Sanz-García J M, López F J and Jaque F 1996 *Phys. Rev.* B **54** 13042
[5] Torchia G A, Sanz-García J A, Diaz-Caro J, Jaque F and Han T P J 1998 *Chem. Phys. Lett.* **65–70** 288
[6] Martín A, López F J and Agulló-López F 1992 *J. Phys.: Condens. Matter* **4** 847
[7] Corradi G, Soethe H, Spaeth J M and Polgar K 1992 *Ferroelectrics* **125** 295
[8] Macfarlane P I, Holliday K, Nicholls J F H and Henderson B 1995 *J. Phys.: Condens. Matter* **7** 9643
[9] Serrano M D, Bermúdez V, Arizmendi L and Diéguez E 2000 *J. Cryst. Growth* **210** 670
[10] Salley G M, Basun S A, Kaplyanskii A A, Meltzer R S, Polgar K and Happek U 2000 *J. Lumin.* **87** 1133
[11] Torchia G A, Sanz-García J A, López F J, Bravo D, García-Sole J, Jaque F, Gallagher H G and Han T P J 1998 *J. Phys.: Condens. Matter* **10** L341
[12] Glass A M 1969 *J. Chem. Phys.* **50** 1501
[13] Camarillo E, Tocho J, Vergara I, Diéguez E, García-Sole J and Jaque F 1992 *Phys. Rev.* B **45** 4600
[14] Abrahams S C and Marsh P 1986 *Acta Crystallogr.* B **42** 1846
[15] Carruthers J R, Peterson G E and Grasso M 1971 *J. Appl. Phys.* **42** 1846
[16] Nevado R, Lifante G, Torchia G A, Sanz-García J A and Jaque F 1998 *Opt. Mater.* **11** 35
[17] Voda M, García-Sole J, Jaque F, Vergara I, Kaminskii A, Mill B and Butashin A 1994 *Phys. Rev.* B **49** 3755
[18] Biernacki S W, Kaminska A, Suchocki A and Arizmendi L 2002 *Appl. Phys. Lett.* **81** 442
[19] Sturge M D and Guggenheim H J 1970 *Phys. Rev.* B **2** 2459